

Technical note

## Interface pressure sensor for IVRA and other biomedical applications

V. Casey<sup>a,\*</sup>, S. O'Sullivan<sup>b</sup>, J.A. McEwen<sup>c</sup>

<sup>a</sup> *Physics Department, University of Limerick, Limerick, Ireland*

<sup>b</sup> *Boston Scientific, Galway, Ireland*

<sup>c</sup> *Western Clinical Engineering Ltd., 544-2660 Oak Street, Vancouver, BC, Canada V6H 3Z6*

Received 20 March 2003; accepted 22 September 2003

### Abstract

The fabrication and testing of a minimally intrusive (2 mm high, 10 mm diameter) biomedical interface pressure sensor are described. Such sensors are needed for the implementation of improved safety features in the next generation of automated intravenous regional anaesthesia (IVRA) systems. The sensor utilizes a structured elastomer as a deflection element sandwiched between the plates of a parallel plate capacitor device. Simple mechanical modifications allow sensitivity and zero offset adjustment. The sensor is housed in a package machined from an engineering polymer. The device is easily calibrated using either a bench-top or an on-body calibration procedure. The device is particularly sensitive to cuff artefacts arising from variations in cuff-wrap tightness and folding of the cuff. As such, it offers some promise for detecting potential hazard conditions which can occur during conventional IVRA procedures.

For the purpose of unit conversion,  $1 \text{ Pa} = 1 \text{ N/m}^2$ ,  $1 \text{ MPa} = 1 \text{ N/mm}^2$  and  $40 \text{ kPa} \approx 300 \text{ mmHg}$ .

© 2003 IPPEM. Published by Elsevier Ltd. All rights reserved.

PACS: 07.07.-a; 07.07.Mp; 46.25.-y; 87.80.-y

Keywords: Non-invasive; Pressure sensor; Biomedical

### 1. Introduction

Intravenous regional anaesthesia (IVRA) is a technique whereby tourniquet cuffs (usually pneumatic) are used to restrict blood flow to a body part such as an exsanguinated limb and retain anaesthetic locally in the limb during surgical procedures. Complications [1] with IVRA are usually pressure related. For instance, nerve injury can occur due to excessive pressures; intraoperative bleeding can occur due to inappropriately low pressure; restricted venous return can occur due to failure to deflate the cuff completely or to remove it from the limb after surgery. Once a pneumatic cuff is wrapped onto a limb and is supported by that limb, it applies either a local or distributed pressure to the limb

that depends upon how snugly it is tied even without inflation. Cuff-applied pressure measurements which rely on air pressure measurements at the compressor, i.e. remote from the cuff, are insensitive to this applied pressure. A snug fit uninflated cuff can easily result in pressures of the order 5–20 mmHg which can impact venous return. Direct measurement devices placed at the cuff/body interface will register this pressure. In addition, the large ‘adjustment’ movement of the cuff which occurs at the lower end of the inflation cycle would suggest that local pressure could vary significantly until such time as uniform intimate contact between the inner wall of the inflating cuff and the tissue is established. Once such contact is established, the cuff hydrostatic pressure is a good indicator of the average interfacial pressure but does not resolve local pressure variations which can occur over bony protrusions or more generally where the local curvature of the limb changes substantially [2,3]. Therefore, there is

\* Corresponding author. Tel.: +353-61-202290; fax: +353-61-202578.

E-mail address: vincent.casey@ul.ie (V. Casey).

a need for an interface pressure sensor system which indicates the actual pressure at a specific location at the tissue/cuff interface in order to avoid many of these pressure-related complications.

There is no agreed functional specification for an interface pressure sensor for surgical tourniquet systems, IVRA systems and other biomedical applications, but an optimal sensor for such applications would conform to the following general specification [5]. Its basic function must be to measure the pressure applied by any one of a specified number of medical devices to a portion of a human body surface, tissue or organ, in the pressure range 0–500 mmHg (0–70 kPa). The sensor design must permit fast, convenient and intuitive calibration checking in the target application environment. Typical errors should be less than  $\pm 2$  mmHg, with hysteresis/creep over a 1-h time period also less than  $\pm 3$  mmHg. In order to be minimally intrusive, the sensor must conform to curved, compliant tissue surfaces with radii of curvature as low as 2 cm (pediatric cuffs) and must not significantly alter the tissue device interface: the sensor must be low profile (<2 mm) with a very small footprint (<1 cm diameter) and have a similar compliance to that of the target tissue. Generally, desirable additional attributes include biocompatibility, immunity to electromagnetic interference (EMI), conformance to relevant electrical standards, and that it must not present electrosurgical or thermal hazards, must fail safe and, for reusable devices, must be sterilizable using at least one of the various conventional sterilization techniques. The performance to cost ratio must be high particularly for disposable devices.

While there have been significant improvements in interface pressure sensors and systems in recent years [6,7], there is still a significant gap [8–10] between desirable performance and actual performance measured against the specification outlined above.

Parallel plate capacitor sensors [11] are particularly interesting for biomedical pressure sensing, as they are inherently planar and are relatively simple to implement. The device capacitance,  $C$ , is given by  $C = \epsilon A/t$ , where  $\epsilon$  is the dielectric constant,  $A$  is the capacitor area and  $t$  is the dielectric thickness, i.e. plate separation. The movement of one electrode (suspended) with respect to the other electrode (fixed) in response to an applied force/pressure changes  $t$  and consequently  $C$  which may be measured and correlated with the applied pressure [4]. The compression ratio,  $\lambda$ , is related to the strain,  $\Delta t/t$ , through

$$\lambda = 1 + \frac{\Delta t}{t} \quad (1)$$

where  $\Delta t$  is the pressure-induced change in dielectric thickness which has an unstrained value  $t_0$ . In a strain-controlled experiment, this simple theory leads one to expect a simple linear relationship between measured

capacitance and  $1/\lambda$ ,

$$C = \frac{\epsilon A}{t_0} \frac{1}{\lambda} \quad (2)$$

since the dielectric thickness for arbitrary strain is  $t = \lambda t_0$ .

Common implementations of such pressure sensors use elastomeric dielectrics as the deflection element sandwiched between the capacitor electrodes. A continuous elastomer layer would not provide the required sensitivity since the surface available for bulging of the elastomer would be extremely small (elastomers are virtually incompressible and so deform through shape rather than volume change). Structured elastomers on the other hand will have a much larger load-free surface area and so will have much larger deformation for a given load. Device sensitivity is directly proportional to the area and to  $1/t^2$  for a given elastomer and so it is desirable to reduce the thickness of the elastomer as much as possible. However, it is difficult to produce low-dimensional elastomer structures in a controlled way using standard electronic production processes such as thick film printing. For this reason, successful devices based upon this approach have evolved in the weighing mat and gait analysis sector, where area restrictions are not so stringent and large area devices can be used to compensate for the loss in sensitivity due to thicker elastomer structures. Such devices are too intrusive for general biomedical applications. Here, we describe a pressure sensor which uses a very thin, 100  $\mu\text{m}$  thick structured elastomer, in a low-profile/low-area capacitive pressure sensor implementation.

## 2. Sensor construction

The overall sensor construction including package is illustrated in Fig. 1. Gold electrodes were printed onto

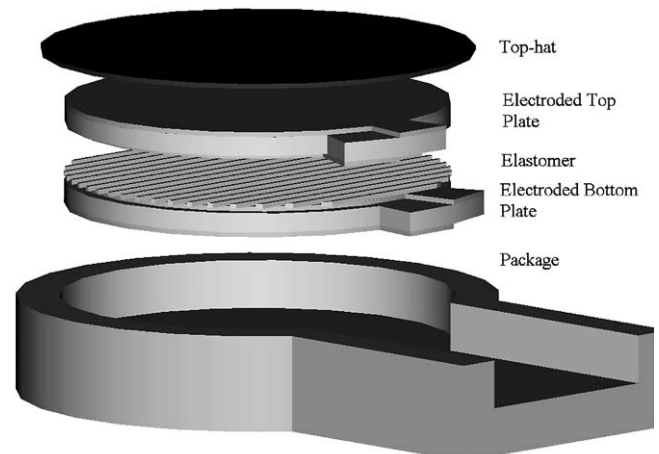


Fig. 1. Sensor and package configuration.

both sides of specially shaped laser scribed alumina substrates (Kyocera, 96% A476) using a thick film process. Lines 100  $\mu\text{m}$  wide were cut using a laser (MCI, Cambridge) in a 100  $\mu\text{m}$  thick piece of stainless steel shim with a 300  $\mu\text{m}$  spacing. This structure was used as a simple transfer mould to form complimentary elastomer (RTV silastic silicone, Dow Corning 9161) structures on one substrate. A second substrate was placed on top of the moulded elastomer. The inner electrodes formed the plates of a parallel plate capacitor with the elastomer as the dielectric, while the outer electrodes were used as the device EMI shield.

Plastic packages offer many advantages over metal or ceramic equivalents for biomedical applications, particularly where low cost and biocompatibility are primary concerns. Common plastics such as perspex and polycarbonate were not sufficiently rigid. Packages formed from the engineering polymer polybutylene terephthalate—30% glass fibre reinforced, Valox (Goodfellow Cambridge Ltd.), were found to work well for the application. The package was shaped with a cable landing area to one side which facilitated cable anchoring and electrical isolation but also allowed mechanical decoupling of the sensor from cable-related strains. The sensor to cable decoupling was achieved using individual gold wires (30  $\mu\text{m}$  diameter) to interconnect between the bonding pads on the sensor and the anchored cable terminations.

The cuff membrane will not in general conformally map the profile of a rigid or semirigid sensor which has been placed between it and tissue to measure the interface pressure. Instead, the cuff will lift away from the sensor top edge and contact the tissue some distance removed from the sensor similar to the way in which a hammock curves between its two support points. A similar effect will occur between the top-plate edge and the package edge if the two are not flush. This so-called ‘hammock’ effect changes the effective pressure sensing area of the device in a complex way as a function of applied pressure and limits the ultimate accuracy and reproducibility of even minimally intrusive deflection type pressure sensors [3] in non-invasive biomedical pressure sensing applications. It was found that satisfactory sensor operation could be achieved by placing a rigid inverted ‘top-hat’ structure which defined a reasonably robust ‘constant area’ for the device, on top of the top-plate. The top-plate area was used as the calibration area for the device. Finally, a thin neoprene rubber membrane preformed in the shape of an open-ended tube was stretched over the entire package plus sensor assembly. In addition to closing the package, this membrane provided a very convenient means of preloading the sensor, i.e. setting the zero force value, by simply adjusting the diameter of the preformed tube.

### 3. Sensor test results

A photomicrograph of the moulded silicone ribs formed on a gold electroded ceramic substrate is shown in Fig. 2. The ribs adhered well to the substrate and were found to be continuous and replicated the basic geometry of the mould, i.e. high aspect ratio ribs separated by polymer-free spaces. Attempts to obtain the same geometry using thick film screen printing invariably resulted in reflow of the uncured polymer into the rib spacing area with consequent loss of the design geometry. The laser cut mould does, however, produce jagged edges on the ribs. In addition, the top surface is not smooth but contains surface protrusions which are likely to affect the low load region of the device since the entire surface of the elastomer ribs will not be in intimate contact with the top electrode until these protrusions have deformed completely. Eight devices (PS1–8) were fabricated using the structure illustrated in Fig. 1. PS1 and PS6 were used to investigate the capacitance/strain relationship for unpackaged devices. The remaining devices were used for bench-top and on-body performance studies.

An unpackaged device (PS6) was placed on the anvil of a solid metal rectangular frame which had a micrometer screw (non-rotating spindle) fitted above the anvil. Device capacitance was recorded as the micrometer position was adjusted to increase the strain on the device. The measured capacitance is plotted against inverse compression ratio ( $1/\lambda$ ), Eq. (2) in Fig. 3. At large strains ( $1/\lambda > 2$ ), the capacitance tends to saturate probably as a consequence of increased stiffness in the elastomer at such high compression ratios, giving an overall non-linear plot. The data from the low strain region ( $1/\lambda < 2$ ) may be fitted to a simple linear relationship, in the capacitance range 4–6.5 pF,

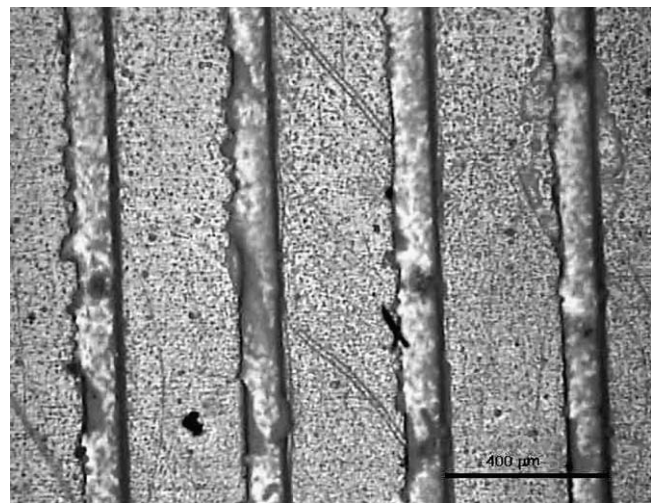


Fig. 2. Magnified image (50 $\times$ ) of the silicone ribs formed on a gold electroded ceramic substrate.

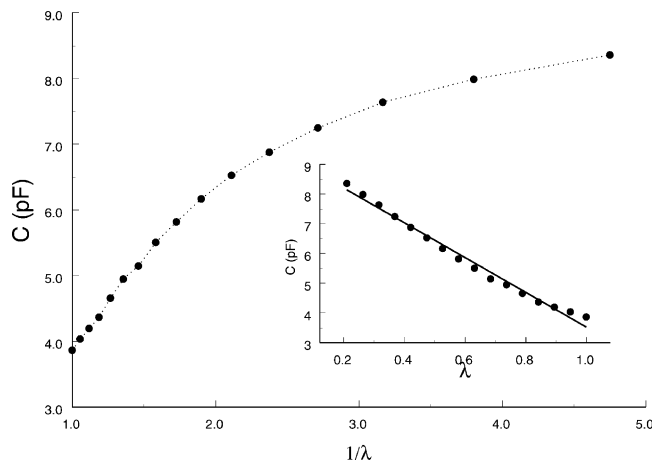


Fig. 3. Capacitance versus  $1/\lambda$  for unpackaged PS6 device. Inset shows same capacitance data plotted against compression ratio,  $\lambda$ .

which, as will be seen later, corresponds roughly to a normal working pressure range of 0–300 mmHg for these devices. It is interesting to note that a plot of capacitance versus  $\lambda$  yields a very good linear fit, see inset of Fig. 3, over the entire range tested, although the physical basis for such a simple relationship is uncertain.

The sensors described here are effectively low-profile load cells in which sensor capacitance is a function of the load applied to the device. Loading them with known weights as in a standard dead-weight-test (DWT) allows convenient pressure calibration of the sensor over any desired range once device area is taken into account. The capacitance versus pressure ( $CP$ ) characteristics shown for PS2 (no zero adjust membrane or top-hat insert) in Fig. 4 were obtained in this way. There is a very large capacitance excursion for the first load increment applied, Fig. 4(a), due to lack of intimate contact between the top electrode and the elastomer, possibly as a result of the surface roughness of the elastomer ribs. Subsequent to this initial excursion, the capacitance increases smoothly with load. Zero stabilization is conveniently achieved by stretching a neoprene membrane over the package so that it presses down upon the top electrode, thereby ensuring intimate contact. This preloading reduces/removes the initial loading excursion. The characteristic with neoprene zero stabilization is shown in Fig. 4(b). The zero load capacitance may be controlled by adjusting the tightness of the membrane through adjustment of the diameter of the neoprene tube used. Bench-top zeroes for the devices were found to be stable to within  $\pm 0.05$  pF ( $\equiv \pm 15$  mmHg) over periods of weeks of active use in the laboratory using this simple approach.

The zero-stabilized device  $CP$  characteristic is still non-linear after zero stabilization. A second order polynomial relationship was found to give the best-fit

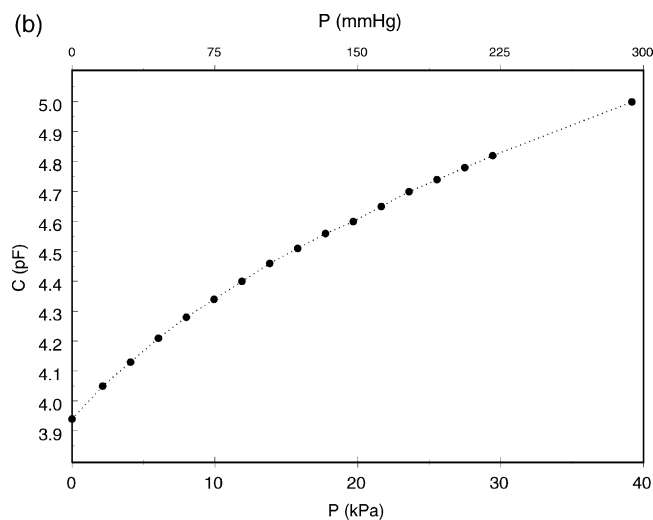
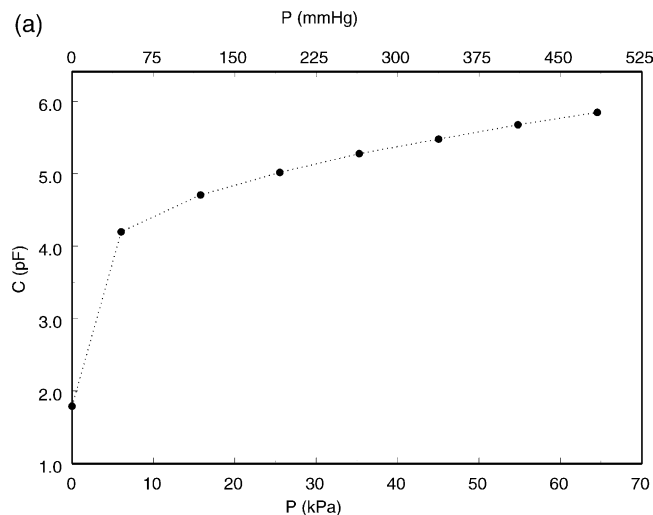


Fig. 4. Capacitance load data for unadjusted and zero adjusted sensor: (a) no zero adjustment, (b) neoprene zero adjustment.

relationship between sensor capacitance,  $C_S$ , and applied pressure,  $P$ ,  $C_S = A + B * P + C * P^2$ . The ratio of the linear coefficient,  $B$ , to the second order coefficient,  $C$ , may be used as an index of the linearity of the characteristic. This ratio is divided by 1000 to yield convenient numbers for comparison. A linearity ratio of greater than 10, determined in this way, is desirable in order to allow the simplest form of calibration, i.e. zero setting and sensitivity adjustment. An estimate of device hysteresis may be made by determining the difference between the load and unload best-fit curves at the mean load/pressure and expressing this as a percentage of the maximum load/pressure used. Zero offset adjustment, i.e. increasing the zero offset from  $\sim 3.5$  to  $\sim 4$  pF, improves the linearity slightly from a value of  $\sim 0.6$  to  $\sim 0.7$  under DWT. However, this reduces sensor sensitivity since overall sensor sensitivity decreases with increasing strain. There is also a small

improvement in device hysteresis, reduced from 2.2% to 1.5%, with zero offset adjustment.

On-body data were obtained by locating the sensor centrally under the cuff. The cuff was inflated to 300 mmHg and deflated to 0 mmHg three times in order to establish a stable location on the limb, as indicated by reproducible capacitance readings for the 300 mmHg datum. Two complete cycles were recorded at each location, as it was found that hysteresis was always lower for the second and subsequent cycles than for the first cycle. The top-hat inserts increase the zero offset ( $A$  coefficient) since they stretch the membrane more, thereby increasing the preload pressure, i.e.  $A$  increases from 4.89 for no top-hat to 5.19 for a 10 mm diameter top-hat. While an increased zero offset would be expected to reduce the sensor sensitivity ( $B$  coefficient), this reduction would appear to be more than compensated by the increase in sensitivity caused by the increased effective area of the sensor due to the insert, i.e.  $B$  increases from  $3.47 \times 10^{-3}$  without top-hat to  $4.79 \times 10^{-3}$  with 10 mm diameter top-hat. The fact that the sensor sensitivity is significantly less, i.e.  $1.89 \times 10^{-3}$  for the DWT data obtained with an 8 mm top-hat insert, supports this view. Using a slightly larger top-hat insert increases the on-body sensor sensitivity further. The inserts give rise to an improvement in linearity of the DWT data, i.e. increase from 1.5 to 3.2. However, the improvement is reduced for on-body data obtained using the same structure, i.e. linearity of 1.5 compared to 0.9 without top-hat. Therefore, marginal improvements in sensitivity and linearity may be achieved through the use of fixed area inserts with these devices. The cost of such improvements is an increased sensor height with correspondingly increased susceptibility to hammocking of the cuff and body tissue about the sensor, thereby making on-body calibration of the device essential.

On-body measurements were made at a range of limb locations using both 17" and 34" Zimmer single-use cuffs for six devices, PS2–5 and PS7 and PS8. Second cycle results obtained for the 17" cuff on the upper and lower arm are shown in Fig. 5. In general, reproducibility of the data at a given location was good. However, there can be substantial variation in data between locations. The difference, for instance, between the lower and upper arm capacitances at 300 mmHg is equivalent to 50 mmHg. This variation in response with location is attributed largely to variation in the folding of the cuff in the vicinity of the sensor and to differences in hammocking at both sites. The lower arm location is relatively stiff compared to the upper arm (biceps) location and so hammocking is expected to be larger in the former case, thereby giving a larger sensor response. Similar variation was found between thigh and calf leg locations, Fig. 6, using the

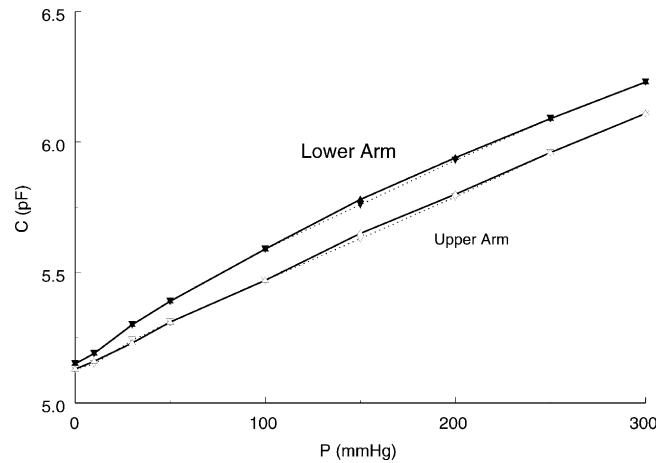


Fig. 5. Second cycle data obtained with the 17" Zimmer cuff for soft tissue locations on the upper and lower arm.

34" cuff. The increased response for the calf location is again attributed to increased hammocking arising from a combination of increased curvature of the limb combined with somewhat stiffer tissue properties. Linearity and hysteresis values were determined from the polynomial regression analysis as above. Variation in the on-body zero value, i.e.  $A$  coefficient, arises because of variability in the initial fit of the cuff to the limb. This value gives a useful indication of the cuff tightness. If the cuff is, in part, or as a whole, resting on the sensor, then an applied pressure will be registered even though the cuff inflation pressure may be zero. As mentioned earlier, the second inflate–deflate cycle results in consistently lower hysteresis values ( $\sim 0.5\%$ ) than the first cycle (1.5–2.1%) at a given measurement location. The on-body data presented in Figs. 5 and 6 are representative of data obtained for all six devices tested.

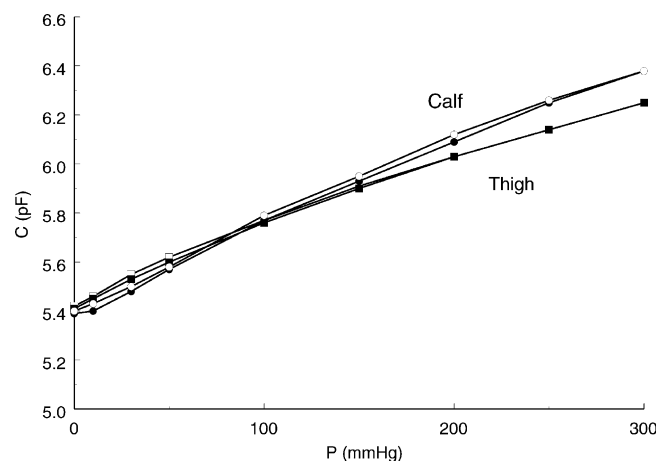


Fig. 6. Second cycle data obtained with the 34" Zimmer cuff for soft tissue locations on the upper and lower leg.

#### 4. Discussion and conclusions

A biomedical pressure sensor incorporating a micro-structured elastomer dielectric as the deflection element in a capacitor type structure is described. By reducing dielectric thickness to micrometer dimensions in a controlled way, device capacitance and sensitivity are increased significantly over devices incorporating thicker dielectrics. This results in lower profile, lower area sensors that are better suited to general non-invasive biomedical applications.

A thin neoprene membrane stretched over the package and electrode assembly may be used to stabilize device zero offset without producing a ‘dead-zone’ in the output characteristic. Top-hat inserts produce marginal improvements in the linearity and sensitivity of the sensor but increase sensor susceptibility to hammocking errors. In general, the cuff will not start to inflate until the gas pressure is high enough to overcome the equivalent pressure applied by the uninflated cuff to the limb. A pressure measurement derived from the hydrostatic pressure in the cuff does not, therefore, reflect the actual applied pressure in this situation. Considerable cuff slippage and relaxation can occur for cuff pressures in the 0–50 mmHg region. Feedback cuff inflation systems mask this effect, as pumping is activated to maintain a constant hydrostatic pressure. The sensor described here will reflect the actual local pressure variations and will indicate the tightness of the uninflated cuff.

Despite reasonable consistency in the readings obtained for a given location in a given measurement sequence, reproducibility is very poor as shifting location or indeed replacement at the same location can result in large changes in indicated pressure. Wrinkling and folding of the inner lining of the cuff may have a strong influence on the sensor response when such wrinkles and folds are in the vicinity of the sensor. The first inflate/deflate cycle at a given location will generally result in hysteresis which is significantly larger than the value which pertains to subsequent cycles. Second and subsequent inflate/deflate cycles will in general have hysteresis values which are less than 1%. Measurement protocols may be devised to minimize some or all of these effects. However, the need for such protocols is indicative of the complexity of the cuff/sensor/tissue interface.

While the device described here meets many of the specifications outlined in the introduction for an optimal biomedical sensor, there are still significant challenges to be overcome in relation to device compliance. The device offers some potential for IVRA systems, as it can provide useful guidance relating to initial cuff tightness and can also serve to indicate fault/alarm

conditions since it directly measures the pressure under the cuff. However, robust calibration of the device for on-body applications is difficult because of the complexity of the interface. While sensor sensitivity may be increased by increasing the area of the device using top-hat inserts, a better strategy probably involves reducing the elastomer thickness even further to increase overall device capacitance/sensitivity. This would allow further reductions in sensor area. Work to this end is continuing at the University of Limerick, where additionally we hope to replace the ceramic substrate and rigid polymer package with flexible options and thereby develop a compliant version of the structure described here.

#### Acknowledgements

This work was funded jointly by Abatis Medical Technologies Limited, Limerick, and the Applied Research Grants Scheme of Enterprise Ireland (Project Ref: HE/97/159).

#### References

- [1] Kumar SN, Chapman JA, Rawlins I. Vascular injuries in total knee arthroplasty. A review of the problem with special reference to the possible effects of the tourniquet. *J Arthroplasty* 1998;13(2):211–6.
- [2] O'Brien SBG, Casey V. Numerical and asymptotic solutions for hammocking. *Q J Mech Appl Math* 2002;55:409–20.
- [3] Casey V, Griffin S, O'Brien SBG. An investigation of the hammocking effect associated with interface pressure measurements using pneumatic tourniquet cuffs. *Med Eng Phys* 2001;23:511–7.
- [4] Neuman MR, Berec A, O'Connor E. Capacitive sensors for measuring finger and thumb tip forces. *IEEE Front Eng Comput Health Care* 1984;436–9.
- [5] Paris-Seeley NL, Romilly DP, McEwen JA. A compliance-independent pressure transducer for biomedical device/tissue interfaces. *Proceedings of RESNA (Rehabilitation Engineering Society of North America Conference)*, Montreal, June. 1995.
- [6] Gyi DE, Porter JM, Robertson NKB. Seat pressure measurement technologies: considerations for their evaluation. *Appl Ergon* 1998;27:85–91.
- [7] Gyi DE, Porter JM. Interface pressure and the prediction of car seat discomfort. *Appl Ergon* 1999;30:99–107.
- [8] Allen V, Ryan DW, Lomax N, Murray A. Accuracy of interface pressure measurement systems. *J Biomed Eng* 1993;15:344–8.
- [9] Buis AWP, Convery P. Calibration problems encountered while monitoring stump/socket interface pressure with force sensing resistors: techniques adopted to minimise inaccuracies. *Prosthet Orthot Int* 1997;21:179–82.
- [10] Polliack AA, Sieh RC, Craig DD, Landsberger A, McNeil DR, Ayyappa E. Scientific validation of two commercial pressure sensor systems for prosthetic socket fit. *Prosthet Orthot Int* 2000;24:63–73.
- [11] Puers R. Capacitive sensors: when and how to use them. *Sens Actuators A* 1993;37–38:93–105.